Testing couplings of three vector bosons through hadron collisions at Fermilab Tevatron energy

Chao-Hsi Chang*
Fermi National Accelerator Laboratory, P.O. Box 500, Batavia, Illinois 60510
and Department of Physics, The University of Michigan, Ann Arbor, Michigan 48109

S. -C. Lee†
Fermi National Accelerator Laboratory, P.O. Box 500, Batavia, Illinois 60510
(Received 26 May 1987)

A test for vector-boson trilinear couplings through hadron collisions at Fermilab Tevatron energy is investigated. The contributions from the standard model to the polarization cross section for W^+W^- pair production process are given and deviations from the standard model are considered. It is pointed out that some effects may be observable in Tevatron collider experiments.

I. INTRODUCTION

Since the weak bosons $W^{\pm}$ and Z^0 were discovered,[1] one of the most interesting problems remaining is to test the couplings of $W^{\pm}$, Z^0, and γ to see if they are of gauged $SU(2)\times U(1)$ symmetry.[2–29] This is important not only for proving the standard model,[30] but also for testing models beyond.[31]

One way to test the three-vector-boson couplings is to focus on experiments at the CERN e^+e^- collider LEP II on the production of charged-weak-boson ($W^{\pm}$) pairs in e^+e^- annihilation, which is related to the couplings of $W^+W^-Z^0$ and $W^+W^-\gamma$. Having relatively high luminosity (5×10^{31} cm^{-2}sec^{-1}) and being in the clean environment of e^+e^-, undoubtedly LEP II will give us a lot of useful information on the couplings. However, since the Fermilab $p\bar{p}$ collider Tevatron has begun to accumulate data, it is worthwhile to investigate the possibilities to test these couplings and to see what kinds of deviations from the standard model are relatively easier to be detected at the Tevatron collider.

Although a hadron collider does not provide a clean environment to test these couplings, besides having at present a relatively low luminosity to work with, there are some advantages. It was pointed out in Ref. 32 that if there are some deviations from the standard model and their effects are proportional to the masses of the fermions in the pair production processes $f\bar{f}\to W^+W^-$, then it is almost impossible for an e^+e^- collider to observe them, while for a hadron collider it is possible due to heavy-quark components in the nucleon structure functions. Another advantage is that in a hadron collider the invariant mass of the W pair can reach a relatively high value. We know that the higher the invariant mass, the easier it becomes to test the gauge cancellation and to see the deviations from gauge couplings if there are any. Therefore, under the Tevatron conditions, how well one can test the couplings of three vector bosons deserves a careful analysis. On the other hand, if one hopes to discover new physics through W^+W^- production, he also needs to know the standard-model contributions as a background and to estimate the contributions from various possible deviations from the standard model. Thus, in this paper we will investigate these problems; i.e., considering the Tevatron conditions, we will compute the W^+W^- production cross sections systematically.

In Ref. 32 the authors pointed out that, due to heavy quarks, all of the most general couplings of the three vector bosons should be considered in hadron collision processes where there are ten types in total, as opposed to what the authors of Refs. 7 and 28 did in the e^+e^- collider case where they could ignore all couplings proportional to the fermion masses. Moreover, in hadron collisions, the Higgs-boson-exchange mechanism is not ignorable either for the same reason. In order to be consistent, we also should consider the general couplings of Higgs bosons to the vector bosons. Thus, in W^+W^- pair production through annihilation of a pair of $q\bar{q}$, in general, 23 types of couplings in total will be relevant. The 23 consist of ten for the W^+W^-Z vertex, seven for $W^+W\gamma$, three for W^+W^-H (here, the Higgs boson H couples to quarks as a scalar), and three for $W^+W^-H_P$ (here the "Higgs boson" H_P couples to quarks as a pseudoscalar). In this paper we will discuss their effects separately in $p\bar{p}$ collision at Tevatron energy.

Being interested in the three-vector-boson couplings, we will not discuss the related mechanisms, such as the equivalent W-boson fusion mechanism and gluon fusion through fermion-loop mechanism, etc.[27,33] Their contributions can be simply added to what we will discuss. Thus, we focus on the W^+W^- pair production through the Drell-Yan mechanism.[34] Owing to such a large number of possible couplings, if one wants to obtain any information on the individual coupling, one has to perform a polarization analysis.[7,8,25,28]

One may imagine that if one keeps all mass terms, the formalism would be complicated, especially with respect to those couplings which would not contribute in the massless limit. However, in fact, we find that the density matrix can be factorized into four terms so the final results are not so complicated.

This paper is organized as follows. In the next section, the most general couplings for $W^+W^-\gamma$, $W^+W^-Z^0$, W^+W^-H, and $W^+W^-H_P$ will be given; the density matrix of polarization for W^+ and W^- are derived. In Sec. III, the formulas of W^+W^- pair production cross sections for $p\bar{p}$ collision are presented. Adopting the Eichten-Hinchliffe-Lane-Quigg (EHLQ) structure functions,[26] and setting the couplings to deviate from those of the standard-model predictions one by one, we compute the numerical values of the polarization cross sections and plot the cross sections against the angle between the proton beam and the produced W boson in the hadron center-of-mass system and against the invariant mass of the W^+W^- pair. In order to compare with the standard model, in every figure we also plot the corresponding standard-model curves. In the last section, Sec. IV, we will discuss our results and draw some conclusions.

II. GENERAL COUPLINGS AND POLARIZATION DENSITY MATRIX

A. General couplings of three vector bosons

The strategy of investigating the couplings for the three-boson vertex in a model-independent way is to start from the most general Lorentz-covariant couplings,

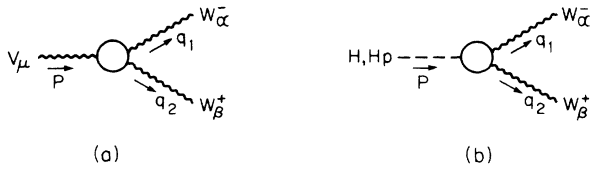

FIG. 1. The three-boson vertex. (a) VW^+W^-. (b) $H_{H_P}W^+W^-$.

which are independent of each other, and then to set each term to a non-standard-model value to see its corresponding consequences. Therefore, we first discuss the most general couplings.

In this paper we restrict ourselves to consider only the W^+W^- pair production; hence, we need the most general couplings for W^-W^+Z and $W^+W^-\gamma$. In Ref. 28 the authors considered the process $e^+e^-\to W^+W^-$ in which the masses of the fermions may be ignored so that only 14 of the most general couplings are effective. (The authors of Ref. 7 had done the same, but as pointed out in Ref. 28, they included two more couplings which are not independent of the rest when fermion masses are neglected.) Aa a matter of fact, the most general couplings for three vector bosons with W^+W^- on shell should involve 17 couplings. They are

$$\Gamma_V^{\alpha\beta\mu}(q_1,q_2,P)=f_1^V(q_1-q_2)^\mu g^{\alpha\beta}-\frac{f_2^V}{m_W^{\,2}}(q_1-q_2)^\mu P^\alpha P^\beta+f_3^V(P^\alpha g^{\mu\beta}-P^\beta g^{\mu\alpha})+if_4^V(P^\alpha g^{\mu\beta}+P^\beta g^{\mu\alpha})$$
$$+if_5^V\epsilon^{\mu\alpha\beta\rho}(q_1-q_2)_\rho-f_6^V\epsilon^{\mu\alpha\beta\rho}P_\rho-\frac{f_7^V}{m_W^{\,2}}(q_1-q_2)^\mu\epsilon^{\alpha\beta\rho\sigma}P_\rho(q_1-q_2)_\sigma+if_8^VP^\mu g^{\alpha\beta}$$
$$-i\frac{f_9^V}{m_W^{\,2}}P^\mu P^\alpha P^\beta-i\frac{f_{10}^V}{m_W^{\,2}}P^\mu\epsilon^{\alpha\beta\rho\sigma}P_\rho(q_1-q_2)_\sigma\ , \tag{2.1}$$

where $\Gamma_V^{\alpha\beta\mu}$ is the vertex of three bosons [Fig. 1(a)],

$$\langle W^-(q_1\lambda_1)W^+(q_2\lambda_2)\,|\,J_V^\mu\,|\,0\rangle$$
$$=e_\alpha(\lambda_1)\bar{e}_\beta(\lambda_2)\Gamma_V^{\mu\alpha\beta}(q_1,q_2,P)\ , \tag{2.2}$$

and V denotes γ or Z^0. Note that f_8^γ vanishes and $f_9^\gamma, f_{10}^\gamma$ are not independent of f_4^γ, f_5^γ due to charge conservation. In fact, even if charge conservation is violated, $f_8^\gamma, f_9^\gamma, f_{10}^\gamma$ will not contribute to $f\bar{f}\to W^+W^-$ at all due to the vector coupling of γ to fermion. Therefore, in Eq. (2.1), these three would not be included in our discussions. Considering $WW\gamma$ and WWZ, we now have 17 couplings f_i^Z $(i=1,2,\ldots,10)$ and f_i^γ $(i=1,2,\ldots,7)$. It is easy to check that these f_i^Z and f_i^γ are independent of each other and, taking into account the on-shell conditions

$$q_1^{\,2}=q_2^{\,2}=m_W^{\,2},\quad (q_1e^{\lambda 1})=(q_2e^{\lambda 2})=0\ , \tag{2.3}$$

there are no more independent couplings.

In addition to what has been shown for the 14 couplings in Ref. 28, we list the C,P,T properties of the seventeen couplings in Table I. In the standard model, non-Abelian gauge invariance gives very strong constraints on the couplings:

$$f_1^V(S)=1+O(\alpha)\ ,$$
$$f_2^V(S)=O(\alpha)\ , \tag{2.4}$$
$$f_3^V(S)=2+O(\alpha)\ ,$$

and the others are either $O(\alpha)$ or higher order in α.

TABLE I. C,P,T properties of vector-boson couplings.

i	1–3	4	5	6,7	8,9	10
P	+	+	−	−	+	−
CP	+	−	+	−	+	−
C	+	−	−	+	+	+

Since we are testing the three-vector-boson couplings (Fig. 1) through the Drell-Yan mechanism[34] [Fig. 2(a)] and we want to keep the heavy-quark mass effects, we also include the related diagram through scalars [Fig. 2(c)]. To test the standard model thoroughly, it is also necessary to test the deviation from the minimum Higgs-boson vector. Therefore, we also generalize the Higgs-boson couplings to the W^+W^- pair. According to the different couplings with or without γ_5 with fermions, the scalar couplings to W^+W^- are denoted as $\Gamma^{\alpha\beta}_{(H)}$, where the scalar couples to fermions without γ_5, and $\Gamma^{\alpha\beta}_{(H_P)}$, where the scalar couples to fermions with γ_5 [Fig. 2(c)]. With the definition of the vertex [Fig. 1(b)]

$$\langle W^-(\lambda_1 q_1)W^+(\lambda_2 q_2)\,|\,J\,|\,0\rangle = e_\alpha(\lambda_1)e_\rho(\lambda_1)\Gamma^{\alpha\beta}_{(H,H_P)}, \tag{2.5}$$

the most general $\Gamma^{\alpha\beta}_{(H)}$ and $\Gamma^{\alpha\beta}_{(Hp)}$ are

$$\Gamma^{\alpha\beta}_{(H)} = f_1^S g^{\alpha\beta} + \frac{f_2^S}{m_W{}^2}P^\alpha P^\beta + \frac{f_3^S}{m_W{}^2}\epsilon^{\alpha\beta\rho\sigma}P_\rho(q_1-q_2)_\sigma \tag{2.6}$$

and

$$\Gamma^{\alpha\beta}_{(H_P)} = if_1^P g^{\alpha\beta} + i\frac{f_2^P}{m_W{}^2}P^\alpha P^\beta + i\frac{f_3^P}{m_W{}^2}\epsilon^{\alpha\beta\rho\sigma}P_\rho(q_q-q_2)_\sigma\ . \tag{2.7}$$

For the standard model,

$$f_1^S = 1+O(\alpha),\quad f_i^S = O(\alpha),\quad f_i^P = O(\alpha)\ . \tag{2.8}$$

It turns out that the contributions from $\Gamma^{\alpha\beta}_{(H,H_P)}$ are relatively small at Tevatron energy except at the peak of resonances in the W^+W^- channel. Therefore, we will not discuss them in this paper, but we still keep them in the formulas so that they can be used to analyze the s-channel resonances.

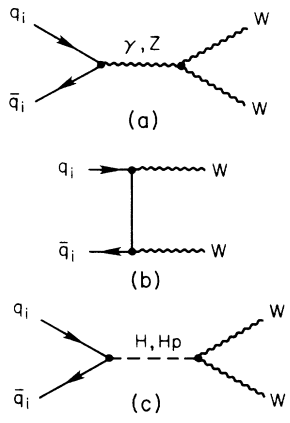

FIG. 2. The Feynman diagrams for $q\bar{q}\to W^+W^-$. (a) The γ- and Z^0-exchange diagram. (b) The t-channel diagram. (c) The scalar-exchange diagram.

B. The polarization density matrix

In order to determine all the couplings in Eq. (2.2), one has to analyze the polarization behavior.

In the hadron collision, the subprocess concerned is $q\bar{q}\to W^+W^-$. To calculate the cross section we need to consider all diagrams in Figs. 2(a)–2(c). According to the Feynman rules we can easily write down the scattering amplitude. Neutral-current and low-energy experiments indicate that the couplings for the vector bosons (γ,Z) to the fermions (quarks and leptons) should be given by those of the standard model. For definiteness we assume the scalars H,H_P couple to the fermions in the same way as the Higgs bosons do in the standard model.

Let $M(k_1\sigma_1,k_2\sigma_2;q_1,\lambda_1,q_2\lambda_2)$ be the scattering amplitude of $q\bar{q}\to W^+W^-$, k_1,k_2, and σ_1,σ_2 are the momenta and helicities of quark and antiquark, respectively, and q_1,q_2 and λ_1,λ_2 are the momenta and polarization, respectively (Fig. 3) for the W bosons. In the paper we will use the rectangular basis $e^\lambda(q)$ for the polarizations of W and use the conventions of Ref. 28 so that $\lambda=1$ labels the transverse polarization in the production plan, $\lambda=2$ labels the transverse polarization perpendicular to the production plane, and $\lambda=3$ labels the longitudinal polarization. The polarization density matrix is defined by

$$\mathcal{P}_{\lambda_1\lambda_2;\lambda_1'\lambda_2'} = \sum_{\sigma_1\sigma_2} M(k_1\sigma_1,k_2\sigma_2;q_1\lambda_1,q_2\lambda_2) \times M^*(k_1\sigma_1,k_2\sigma_2;q_1\lambda_1',q_2\lambda_2')\ . \tag{2.9}$$

Through a straightforward calculation, $\mathcal{P}_{\lambda_1\lambda_2;\lambda_1'\lambda_2'}$ can be factorized into four terms:

$$\mathcal{P}_{\lambda_1\lambda_2;\lambda_1'\lambda_2'} \equiv 2e^4\tilde{\mathcal{P}}_{\lambda_1\lambda_2;\lambda_1'\lambda_2'}\ , \tag{2.10}$$

$$\tilde{\mathcal{P}}_{\lambda_1\lambda_2;\lambda_1'\lambda_2'} = R^v_{\lambda_1\lambda_2}R^{v*}_{\lambda_1'\lambda_2'} + R^a_{\lambda_1\lambda_2}R^{a*}_{\lambda_1'\lambda_2'} + S^v_{\lambda_1\lambda_2}S^{v*}_{\lambda_1'\lambda_2'} + S^a_{\lambda_1\lambda_2}S^{a*}_{\lambda_1'\lambda_2'}\ , \tag{2.11}$$

where $R^{v,a}_{\lambda_1\lambda_2}$ and $S^{v,a}_{\lambda_1\lambda_2}$ are 3×3 matrices. Here, and later on, the asterisk indicates the complex conjugate. Because the couplings of $W^+W^-\gamma$ and W^+W^-Z appear in the matrices with certain combinations, we define the quantities

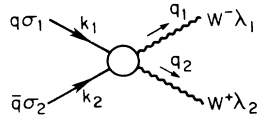

FIG. 3. $q\bar{q}\to W^+W^-$ process and its momentum assignment.

$$a_n = Q_i \left[f_n^{\gamma} - \frac{s}{s - {m_Z}^2} f_n^z \right] ,$$

$$b_n = - \left[\frac{L_i - R_i}{2 \sin^2\theta_W} \frac{s}{s - {m_Z}^2} f_n^z \right], \quad n = 1, \ldots, 10 , \tag{2.12}$$

$$b = \frac{1}{4 \sin^2\theta_W} \sum_I^s \frac{s \mid V_{iI} \mid^2}{t - {m_I}^2} , \tag{2.12a}$$

$$b_m^{S,P} = \frac{1}{2 \sin^2\theta_W} \frac{s}{s - {m_H}^2 - i \Gamma_H m_H} f_m^{S,P}, \quad m = 1,2,3 , \tag{2.12b}$$

where Q_i are the electric charge of the incoming quark, L_i, R_i their left and right weak charge

$$L_i = \tau_i^3 - 2 Q_i \sin^2\theta_W, \quad R_i = -2 Q_i \sin^2\theta_W , \tag{2.12c}$$

m_I are the masses of the corresponding t-channel quarks, V_{iI} are the Kobayashi-Maskawa-Cabibbo (KMC) quark mixing matrix elements, and m_H and Γ_H are the mass and widths of the neutral scalars.

The matrices R^v, R^a, S^v, and S^a have the properties

$$A_{12} = A_{21}^*, \quad A_{13} = -A_{31}^*, \quad A_{23} = -A_{32}^* , \tag{2.13}$$

where A represents any one of R^v, R^a, S^v, S^a matrices and $a_n, b_n, b, b_m^{S,P}$ are treated as real quantities. The matrix elements of R^v, R^a, S^v, and S^a for the down-type incoming quarks are

$$R_{11}^v = \left[(a_1 - \tfrac{1}{2} b_1) \beta_W - b (\beta_W - \beta_i \cos\theta) + \frac{b}{2} \beta_W \right] \sin\theta ,$$

$$R_{12}^v = \left[-2(2a_7 - b_7) \beta_W{}^2 \gamma_W{}^2 - (a_6 - \tfrac{1}{2} b_6) + \frac{i}{2} \beta_i{}^2 b \right] \sin\theta ,$$

$$R_{13}^v = -\tfrac{1}{2} \gamma_W [(2a_- - b_-) \beta_W \cos\theta + \beta_i (b_5 \beta_W{}^2 + i b_6) + b \beta_i \beta_W (\beta_W - \beta_i \cos\theta) - b \cos\theta (\beta_W - \beta_i \cos\theta) - b \beta_i \sin^2\theta] ,$$

$$R_{22}^v = \left[-(a_1 - \tfrac{1}{2} b_1) \beta_W + \frac{b}{2} \beta_W \right] \sin\theta , \tag{2.14}$$

$$R_{23}^v = -\frac{i}{2} \gamma_W \{ b_- \beta_i \beta_W + [(2a_5 - b_5) \beta_W{}^2 + i (2a_6 - b_6)] \cos\theta + b [\beta_W (\beta_i - \beta_W \cos\theta) + \beta_i (\beta_W - \beta_i \cos\theta)] \} ,$$

$$R_{33}^v = \left[-(a_1 - \tfrac{1}{2} b_1) \beta_W (2\gamma_W{}^2 - 1) + 2(2a_2 - b_2) \beta_W{}^3 \gamma_W{}^4 + (2a_3 - b_3) \beta_W \gamma_W{}^2 + \frac{b}{2} \beta_W \left[\frac{2\gamma_W{}^2}{\gamma^2} - 1 \right] \right.$$
$$\left. - b \gamma_W{}^2 (\beta_W - \beta_i \cos\theta) \right] \sin\theta ;$$

$$R_{11}^a = \left[-\tfrac{1}{2} b_1 \beta_W - b (\beta_W - \beta_i \cos\theta) + \frac{b}{2} \beta_W \right] \beta_i \sin\theta, \quad R_{12}^a = \left[\tfrac{1}{2} (4 b_7 \beta_W{}^2 \gamma_W{}^2 + b_6) + \frac{ib}{2} \right] \beta_i \sin\theta ,$$

$$R_{13}^a = \tfrac{1}{2} \gamma_W [b_- \beta_i \beta_W \cos\theta + (2a_5 - b_5) \beta_W{}^2 + i (2a_6 - b_6) - b (\beta_W - \beta_i \cos\theta)^2 + b \beta_i{}^2 \sin^2\theta] ,$$

$$R_{22}^2 = \tfrac{1}{2} (b_1 + b) \beta_W \beta_i \sin\theta , \tag{2.15}$$

$$R_{23}^a = \frac{i}{2} \gamma_W [(2a_- - b_-) \beta_W + (b_5 \beta_W{}^2 + i b_6) \beta_i \cos\theta - b \beta_i \beta_W (\beta - \beta_W \cos\theta) - b (\beta_W - \beta_i \cos\theta)] ,$$

$$R_{33}^a = [\tfrac{1}{2} b_1 \beta_W (2\gamma_W{}^2 - 1) - 2 b_2 \beta_W{}^3 \gamma_W{}^4 - b_3 \beta_W \gamma_W{}^3 - \tfrac{1}{2} b \beta_W - b \gamma_W{}^2 (\beta_W - \beta_i \cos\theta)] \beta_i \sin\theta ;$$

$$S_{11}^v = \frac{1}{2\gamma_i} [-\beta_i b_1^S - (2a_1 - b_1) \beta_W \cos\theta - b (\beta_i - \beta_W \cos\theta) + 2 b \beta_i{}^2 \sin^2\theta] ,$$

$$S_{12}^v = \frac{1}{2\gamma_i} \{ [2a_6 - b_6 + 2(2a_7 - b_7) \beta_W{}^2 \gamma_W{}^2] \cos\theta + 4 b_3^S \beta_i \beta_W \gamma_W{}^2 \} ,$$

$$S_{13}^v = \frac{\gamma_W}{2\gamma_i} [(2a_- - b_-) \beta_W - 2b (\beta_W - \beta_i \cos\theta) + b \beta_W] \sin\theta ,$$

$$S_{22}^v = \frac{1}{2\gamma_i} [\beta_i b_1^S + (2a_1 - b_1) \beta_W \cos\theta + b (\beta_i - \beta_W \cos\theta)] = -S_{11}^v + \frac{b}{\gamma_i} \beta_i{}^2 \sin^2\theta , \tag{2.16}$$

$$S_{23}^v = -\frac{i \gamma_W}{2\gamma_i} [(2a_5 - b_5) \beta_W{}^2 + i (2a_6 - b_6) - b \beta_W{}^2] \sin\theta ,$$

$$S^v_{33}=\frac{1}{2\gamma_i}\{\beta_i[b^S_1(2\gamma_W{}^2-1)-4b^S_2\beta_W{}^2\gamma_W{}^4]+[(2a_1-b_1)(2\gamma_W{}^2-1)-4(2a_2-b_2)\beta_W{}^2\gamma_W{}^4]\beta_W\cos\theta$$
$$-2(2a_3-b_3)\gamma_W{}^2\beta_W\cos\theta+b(2\gamma_W{}^2-1)(\beta_i-\beta_W\cos\theta)+2b\gamma_W{}^2(\beta_W-\beta_i\cos\theta)\cos\theta\}\ ;$$

$$S^a_{11}=-\frac{1}{2\gamma_i}[(4\gamma_Z{}^2-1)b_8+b^P_1]\ ,$$

$$S^a_{12}=\frac{1}{2\gamma_i}[(4\beta_W\gamma_W{}^2b_{10}-b_5\beta_W)(4\gamma_Z{}^2-1)+4\beta_W\gamma_W{}^2b^P_3+b(\beta_W-\beta_i\cos\theta)]\ ,$$

$$S^a_{13}=-\frac{i\gamma_W}{2\gamma_i}b\beta_i\beta_W\sin\theta,\quad S^a_{22}=-S^a_{11}\ , \tag{2.17}$$

$$S^a_{23}=-\frac{\gamma_W}{2\gamma_i}b\beta_i\sin\theta\ ,$$

$$S^a_{33}=\frac{1}{2\gamma_i}\{[b_8(2\gamma_W{}^2-1)-4b_9\beta_W{}^2\gamma_W{}^4-2b_4\beta_W{}^2\gamma_W{}^2](4\gamma_Z{}^2-1)+b^P_1(2\gamma_W{}^2-1)-4b^P_2\beta_W{}^2\gamma_W{}^4\}\ ,$$

where $\gamma_i,\gamma_W,\gamma_Z,\beta_i,\beta_W,\beta_z$ are, as usual,

$$\gamma_W=\left[\frac{\hat{s}}{2m_W}\right]^{1/2},\quad \beta_W=\left[1-\frac{4m_W{}^2}{\hat{s}}\right]^{1/2},\ \text{etc.}\ , \tag{2.18}$$

and $a_-=a_3-ia_4$, $b_-=b_3-ib_4$. For up-type quarks, the density matrix is again given by Eqs. (2.10) and (2.11) with the following changes. In Eqs. (2.12a) (through t), (2.14), (2.15), (2.16), and (2.17), θ should be changed into $\pi-\theta$; the matrices $R^{v,a},S^{v,a}$ should be transposed $(R,S\to\tilde{R},\tilde{S})$; the signs of f^V_n for $n=1,2,3,6,7$ should be flipped; the up-type quark masses in Eq. (2.12a) should be substituted with the down-type quark masses and the down-type charges in Eq. (2.12) should be substituted with the up-type charges.

Now we are ready to derive the cross sections. In the following section we shall use $\hat{s}$ for the parton c.m. energy squared and s for the corresponding quantity of the incoming hadrons.

III. FORMULAS OF W^+W^- PAIR PRODUCTION CROSS SECTIONS AND NUMERICAL RESULTS

A. Formulas of W^+W^- pair production cross sections

From the density matrix, it is straightforward to obtain the corresponding differential cross section for polarized W^+ and W^- in the parton subprocess $q_i\bar{q}_i\to W^+W^-$:

$$\left[\frac{d\sigma}{d\cos\theta^*}\right]_{\lambda_1\lambda_2;\lambda_1'\lambda_2'}=\frac{\pi\alpha^2\beta_W}{4\hat{s}\beta_i}\tilde{\mathcal{P}}_{\lambda_1\lambda_2;\lambda_1'\lambda_2'}(\theta^*,\sqrt{\hat{s}})\ , \tag{3.1}$$

where θ^* is the angle between the W^- and the incoming hadron A in the hadron center-of-mass system. It follows from the factorization theorem for Drell-Yan processes[35] that the W^+W^- polarization cross section for $AB\to W^+W^-$ (where $A=p$, $B=\bar{p}$ for Tevatron) can be written as

$$\left[\frac{d\sigma}{dMd\cos\theta^*dy_+}\right]_{\lambda_1\lambda_2;\lambda_1'\lambda_2'}=\frac{\pi\alpha^2\beta_W}{sMN_c}\sum_j\left[\frac{1}{\beta_j{}^2}\cosh y_+-\sinh y_+\right][f^A_j(x_a,M^2)f^B_{\bar{j}}(x_b,M^2)\tilde{\mathcal{P}}_{\lambda_1\lambda_2;\lambda_1'\lambda_2'}(\theta^*,M)$$
$$+f^A_{\bar{j}}(x_a,M^2)f^B_j(x_b,M^2)\tilde{\mathcal{P}}_{\lambda_1\lambda_2;\lambda_1'\lambda_2'}(\pi+\theta^*,M)]\ , \tag{3.2}$$

where $N_c=3$ is the color factor; $j=u$, c, t and d,s,b; $M=\sqrt{\hat{s}}$; $f^A_{j(\bar{j})}$ and $f^B_{\bar{j}(j)}$ are the parton distribution functions for parton j $(\bar{j})$ in hadron A and $\bar{j}$ (j) in hadron B and

$$y_+=\tfrac{1}{2}(y_1+y_2)\ . \tag{3.3}$$

Here y_1 and y_2 are the rapidities, in the hadron c.m. frame, of W^- and W^+, and they are related to θ^* as

$$\beta_W\cos\theta^*=\tanh\tfrac{1}{2}(y_1-y_2)\ . \tag{3.4}$$

The effects of the polarizations of W^+W^- can be seen

through the correlations of their decay products. This has been discussed extensively by Hagiwara *et al.* in Ref. 28, in the event when the masses of the final-state fermions can be neglected. Although we shall discuss primarily the polarization cross sections as given in Eq. (3.2), we give below the decay matrices for completeness.

Let $M_2(q_1,\lambda_1;p_1\sigma_1,p_2\sigma_2)$ be the amplitude for the decay of W^- into fermions of momenta p_1,p_2 and helicities σ_1,σ_2. Similarly, let $M_3(q_2,\lambda_2;p_3\sigma_3,p_4\sigma_4)$ be the corresponding quantity for W^+. We use θ_1,ϕ_1 to denote the polar and azimuthal angles of the down-type quark (lepton) in W^- decay and in the W^- rest frame. We use θ_3,ϕ_3 for the corresponding angles in W^+ decay (and in the W^+ rest frame). The decay matrix $D_{\lambda\lambda'}$ is defined by

$$D_{\lambda_1\lambda_1'}=\sum_{\sigma_1,\sigma_2} M_2(q_1\lambda_1;p_1\sigma_1,p_2\sigma_2)M_2^*(q_1\lambda_1';p_1\sigma_1,p_2\sigma_2) . \tag{3.5}$$

$\bar{D}_{\lambda_2\lambda_2'}$ for W^+ decay is defined similarly. One can show that

$$D_{\lambda\lambda'}=\frac{e^2}{2\sin^2\theta_W}|V_{iI}|^2c_-^2\sum_{\sigma_1,\sigma_2}(p_1^0-\sigma_1|\mathbf{p}_1|)\times(p_2^0+\sigma_2|\mathbf{p}_2|)l_\lambda l_{\lambda'}^* , \tag{3.6}$$

where

$$\begin{aligned} l_1&=\cos\theta_1\cos\phi_1+\frac{i}{2}(\sigma_1-\sigma_2)\sin\phi_1 ,\\ l_2&=\cos\theta_1\sin\phi_1-\frac{i}{2}(\sigma_1-\sigma_2)\cos\phi_1 ,\\ l_3&=\sin\theta_1 . \end{aligned} \tag{3.7}$$

Similarly,

$$\bar{D}_{\lambda\lambda'}=\frac{e^2}{2\sin^2\theta_W}|V_{iI}|^2c_+^2\sum_{\sigma_3,\sigma_4}(p_3^0+\sigma_3|\mathbf{p}_3|)\times(p_4^0-\sigma_4|\mathbf{p}_4|)\bar{l}_\lambda\bar{l}_{\lambda'}^* , \tag{3.8}$$

where

$$\begin{aligned} \bar{l}_1&=\cos\theta_3\cos\phi_3+\frac{i}{2}(\sigma_3-\sigma_4)\sin\phi_3 ,\\ \bar{l}_2&=\cos\theta_3\sin\phi_3+\frac{i}{2}(\sigma_3-\sigma_4)\cos\phi_3 ,\\ \bar{l}_3&=\sin\theta_3 . \end{aligned} \tag{3.9}$$

In these formulas, c_-,c_+ are color factors and equal 1 ($\sqrt{3}$) for lepton (quark) final state. If we neglect the masses of the final-state fermions, it is easily seen that $\sigma_1,\sigma_2,\sigma_3,\sigma_4$ can take only a particular value so that the summations over σ_i reduces to one term and we get the result of Ref. 28.

Equations (3.5) and (3.8) can be combined with Eq. (3.2) to give the complete cross sections for decay correlations. We shall postpone a detailed analysis of such correlations as was done in Ref. 28 for e^+e^- collisions, but rather analyze the polarization channels and the kinematical regions (θ^* and M) where a certain deviation from the standard-model predictions is most easily found. For this purpose we shall limit our discussions to the diagonal elements of Eq. (3.2).

For a given invariant mass M and the rapidity y_+ of the W^+W^- pair, the fractions x_a,x_b of hadron momenta carried by the incoming partons in hadron A and hadron B are fixed to be

$$\begin{aligned} x_a&=\sqrt{\tau}(\beta_j\cosh y_+ +\sinh y_+) ,\\ x_b&=\sqrt{\tau}(\beta_j\cosh y_+ -\sinh y_+) , \end{aligned} \tag{3.10}$$

where $\sqrt{\tau}=M/\sqrt{s}$.

We shall integrate over y_+ with the following cuts. Kinematically it is constrained by $0\le x_a,x_b\le 1$. We put in the rapidity cuts of $|y_1|\le 2.5$, $|y_2|\le 2.5$ for W^- and W^+. Finally, since the mass of top quark is set at 70 GeV, which is comparable to the W mass, x_a and x_b for $t\bar{t}$ parton processes can be smaller than 10^{-4}, the limit of validity of the EHLQ structure functions which we are using. Moreover, so far as we know, there is still no completely satisfactory way of taking into account the heavy-quark masses in the parton distribution functions.[26,36] To avoid the problem of small x, we put in the cuts $x_a,x_b\ge\tau$ which are satisfied automatically if the masses of the partons are neglected. Such cuts reduce the t-quark effective luminosity, but has very little effect on the luminosities of other quarks. At Tevatron energy, the differential cross sections are not sensitive to such cuts since the top luminosity is small anyway.

As pointed out above, taking $\lambda_1=\lambda_1'$, $\lambda_2=\lambda_2'$, we have the polarized W^+W^- double differential cross section

$$\left[\frac{d\sigma}{dM\,d\cos\theta^*}\right]_{\lambda_1\lambda_2}=\frac{\pi\alpha^2\beta_W}{3Ms}\sum_j\int dy_+\left[\frac{1}{\beta_j^2}\cosh^2 y_+-\sinh^2 y_+\right][f_j^A(x_a,M^2)f_{\bar{j}}^B(x_b,M^2)\tilde{\mathcal{P}}_{\lambda_1\lambda_2;\lambda_1\lambda_2}(\theta^*,M)+f_{\bar{j}}^A(x_a,M^2)f_j^B(x_b,M^2)\tilde{\mathcal{P}}_{\lambda_1\lambda_2;\lambda_1\lambda_2}(\pi+\theta^*,M)] \tag{3.11}$$

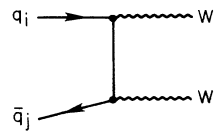

FIG. 4. Feynman diagram for $q_i\bar{q}_j \to WW$ $(i \neq j)$.

where the integration over y_+ is restricted by the kinematic cutoff we chose as explained above.

B. Numerical results

In our numerical calculations, the EHLQ structure function (set 2, $\Lambda = 290$ MeV) (Ref. 26) is used and the parameters are chosen as

$$\begin{aligned} &m_W = 81.8 \text{ GeV}, \quad \sin^2\theta_W = 0.226, \quad \sqrt{s} = 2 \text{ TeV}, \\ &m_u = 3 \text{ MeV}, \quad m_d = 5 \text{ MeV}, \quad m_s = 150 \text{ MeV}, \\ &m_c = 1.5 \text{ GeV}, \quad m_b = 5.5 \text{ GeV}, \\ &m_t = 70 \text{ GeV}, \quad M_H = 400 \text{ GeV}, \quad \Gamma_H = 30 \text{ GeV}. \end{aligned} \tag{3.12}$$

The KMC matrix is taken to be

$$\begin{bmatrix} V_{ud} & V_{us} & V_{ub} \\ V_{cd} & V_{cs} & V_{cb} \\ V_{td} & V_{ts} & V_{tb} \end{bmatrix} = \begin{bmatrix} 0.975 & 0.222 & 0.009\,54 \\ 0.221 & 0.9644 & 0.1455 \\ 0.0231 & -0.144 & 0.9893 \end{bmatrix}. \tag{3.13}$$

Here we ignore the CP phase, but insist on unitarity.

The mass of the Higgs-boson scalar (and that of H_P) is arbitrarily chosen to be 400 GeV with the corresponding width Γ_H (Ref. 26) just to show a typical resonance behavior. As we shall find out, they have very little effect at Tevatron energy.

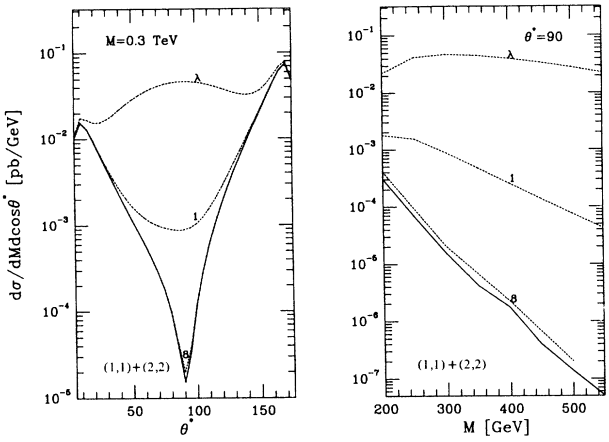

FIG. 6. $d\sigma/dm\, d\cos\theta^*$ for (1,1) + (2,2) polarization channel; solid line is for standard model; dotted lines numbered by 1 and λ are for f_1^Z, f_8^Z, and λZ, respectively, with deviations from their standard-model values by 1.

In order to see the various couplings' contributions we plot our results according to the polarization channels and consider the anomalous $W^+W^-\gamma$ and $W^+W^-Z^0$ couplings separately. In order to facilitate comparison with the standard model we plot our results of the standard model with a solid line. One point which we should note is that in the standard model we should consider the contributions from different flavors $i \neq j$ through the diagram, Fig. 4. However, because of the small KMC matrix mixing and/or the small quark-mass difference, this mechanism, in fact, contributes little to the W^+W^- production at Tevatron energy. It is lower than others by at least an order of magnitude over the entire kinematical region we considered so that it can be safely ignored. In the figures, the numbers which ac-

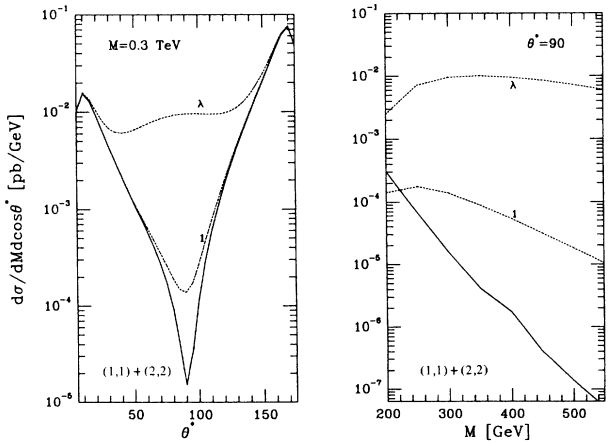

FIG. 5. $d\sigma/dm\, d\cos\theta^*$ for (1,1) + (2,2) polarization channel; solid line is for standard model; dotted lines numbered by 1 and λ are for $f\gamma$ and $\lambda\gamma$, respectively, with deviation from their standard-model values by 1.

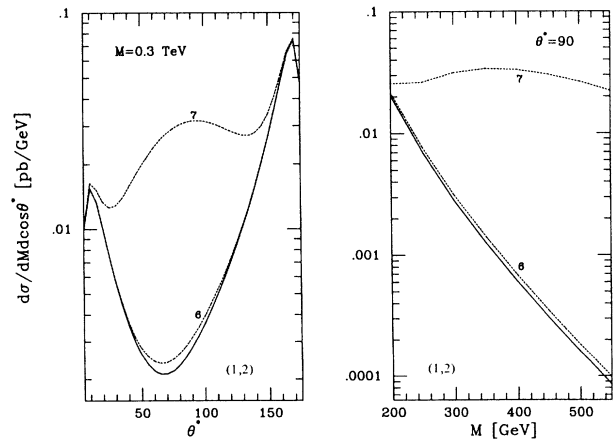

FIG. 7. $d\sigma/dm\, d\cos\theta^*$ for (1,2) + (2,1) polarization channel; solid line is for standard model; dotted lines numbered by 6 and 7 are for $f\zeta$ and $f\gamma$, respectively, with deviations from their standard-model values by 1.

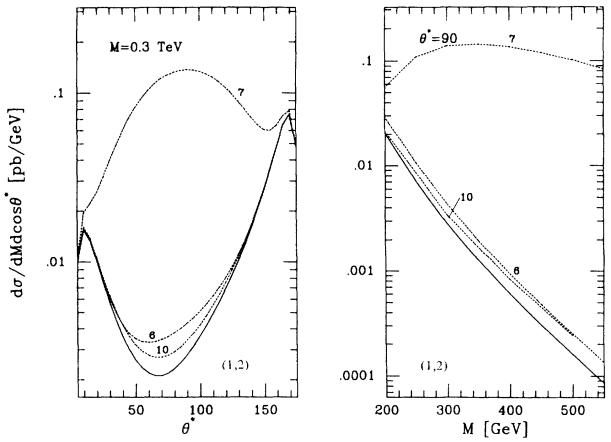

FIG. 8. $d\sigma/dm\, d\cos\theta^*$ for (1,2) + (2,1) polarization channel; solid line is for standard model; dotted lines numbered by 6, 7, and 10 are for f_6^Z, f_7^Z, and f_{10}^Z, respectively, with deviations from their standard-model values by 1.

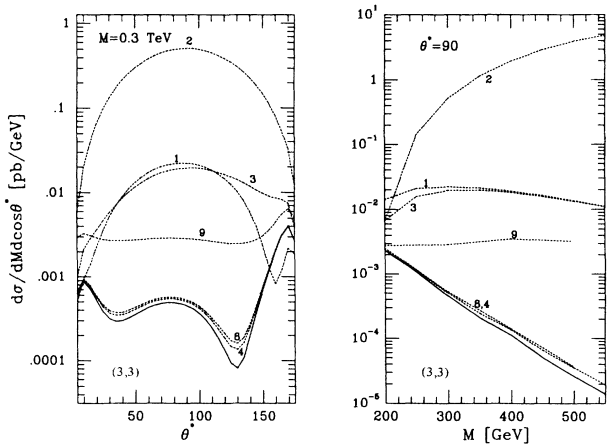

FIG. 10. $d\sigma/dm\, d\cos\theta^*$ for (3,3) polarization channel; solid line is for standard model; dotted lines numbered by 1, 2, 3, 4, 8, and 9 are for f_1^Z, f_2^Z, f_3^Z, f_4^Z, f_8^Z, and f_9^Z, respectively, with deviations from their standard-model values by 1.

company the dotted lines denote the corresponding coupling which deviates from the standard model by one unit and which contributes to the cross sections of the given channel as indicated in the figure. In order to see the angle and energy dependences and to estimate the total events, we put the two graphs together in a figure. We plot the angular distribution by taking the invariant mass of the W^+W^- pair equal to 0.3 TeV. On the other hand, we plot the dependence on the invariant mass of the W^+W^- production by taking a suitable angle to dramatize the variance with M changing.

In Refs. 2–19 and 29, the so-called "anomalous" moment κ_λ of W has been discussed a lot, which corresponds to the f_3^γ deviation. We also plot the λ_V term contributions, which are marked with λ in the figures. The λ_V term is quite similar to the anomalous moment term. In space-time representation, the anomalous moment term is $W_\mu^+ W_\nu V^{\mu\nu}$, but the λ_V term is $W_{\rho\mu}^+ W_\nu^\mu V^{\nu\rho}$, where W_μ is the vector potential of W, $W_{\mu\nu}$ and $V_{\mu\nu}$ are the field strength tensors of W and γ (or Z^0), respectively. They are related to the magnetic moment μ_W and the electric quadrupole moment Q_W of W by

$$\mu_W = \frac{e}{2m_W}\ (1+\kappa_\gamma+\lambda_\gamma)\ ,$$
$$Q_W = -\frac{e}{m_W{}^2}\ (\kappa_\gamma-\lambda_\gamma)\ . \tag{3.14}$$

In standard model, $\kappa_V=1$ and $\lambda_V=0$ at the tree level. f_1, κ, and λ are the only allowed form factors if one in-

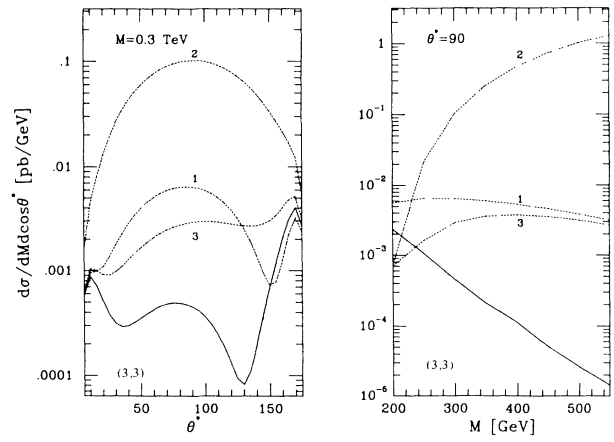

FIG. 9. $d\sigma/dm\, d\cos\theta^*$ for (3,3) polarization channel; solid line is for standard model; dotted lines numbered by 1, 2, and 3 are for f_1^γ, f_2^γ, and f_3^γ, respectively, with deviation from their standard-model values by 1.

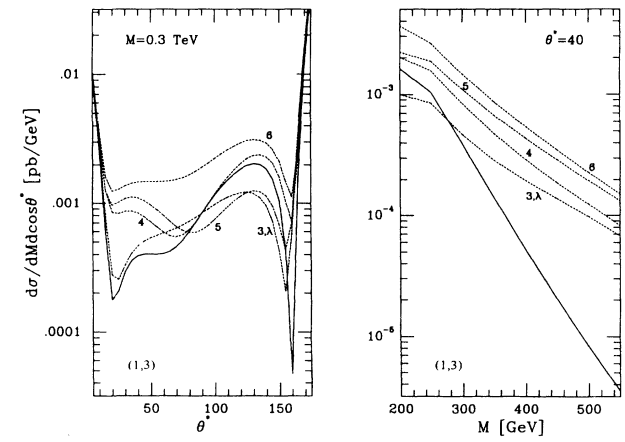

FIG. 11. $d\sigma/dm\, d\cos\theta^*$ for (1,3) + (3,1) polarization channel; solid line is for standard model; dotted lines numbered by 3, 4, 5, 6, and λ are for f_3^γ, f_4^γ, f_5^γ, f_6^γ, and $\lambda\gamma$, respectively, with deviations from their standard-model values by 1.

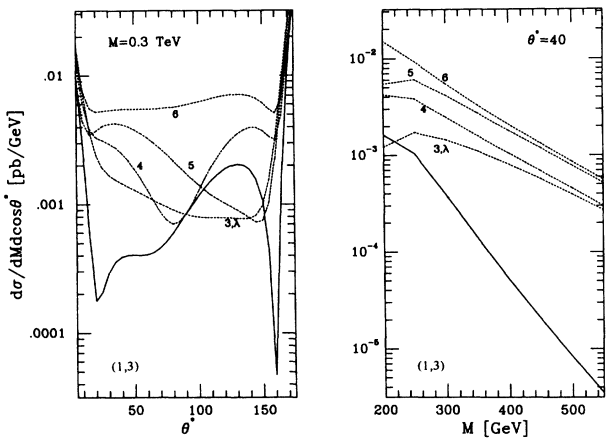

FIG. 12. $d\sigma/dm\, d\cos\theta^*$ for (1,3) + (3,1) polarization channel; solid line is for standard model; dotted lines numbered by 3, 4, 5, 6, and λ are for f_3^Z, f_4^Z, f_5^Z, f_6^Z, and λz, respectively, with deviations from their standard-model values by 1.

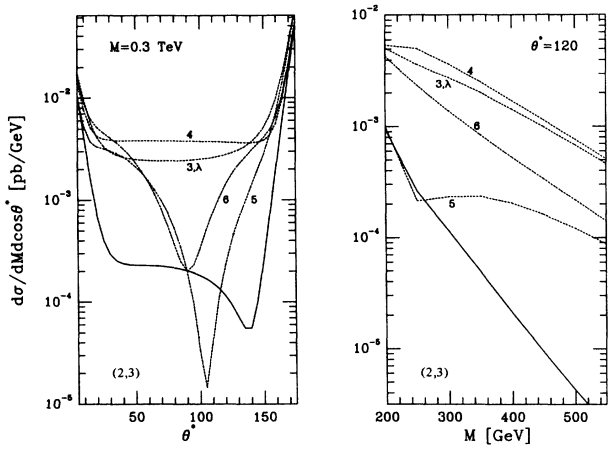

FIG. 14. $d\sigma/dm\, d\cos\theta^*$ for (2,3) + (3,2) polarization channel; solid line is for standard model; dotted lines numbered by 3, 4, 5, 6, and λ are for f_3^Z, f_4^Z, f_5^Z, f_6^Z, and λz, respectively, with deviations from their standard-model values by 1.

sists on global SU(2) invariance upon switching off electromagnetism.[24,31]

Owing to the relation in Eq. (2.13), the magnitude of channels (12) and (21), (13) and (31), (23) and (32) are equal; hence, we plot only their sum. Similarly, as one can see from Eqs. (2.14)–(2.17), the difference in (11) and (22) channels is down by a power of γ_W^2 compared to their sum so that we plot their sum only.

Finally, we note that Figs. 5, 7, 9, 11, and 13 are for the form factors f_i^γ $(i=1,\ldots,7)$ and Figs. 6, 8, 10, 12, and 14 are for the form factors $f_i^Z (i=1,\ldots,10)$.

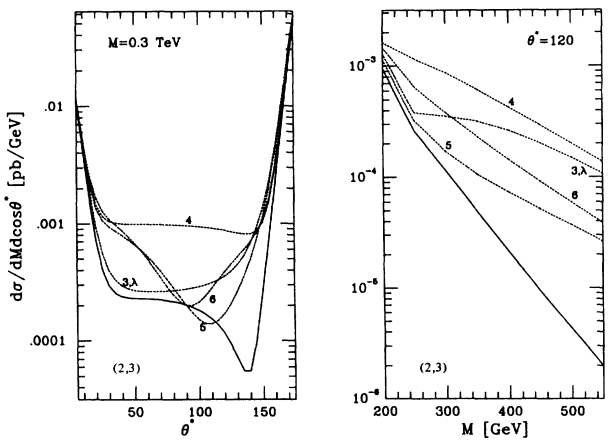

FIG. 13. $d\sigma/dm\, d\cos\theta^*$ for (2,3) + (3,2) polarization channel; solid line is for standard model; dotted lines numbered by 3, 4, 5, 6, and λ are for f_3^γ, f_4^γ, f_5^γ, f_6^γ, and λγ, respectively, with deviation from their standard-model values by 1.

IV. DISCUSSIONS AND CONCLUSIONS

By examining the figures we can easily see the following features. Firstly, in standard model, the production cross section of W pairs in the central region (say $60° \le \theta^* \le 120°$) drop rapidly as the invariant mass M increase. The major contribution comes from the (12) transverse channel which originates from t-channel-exchange diagrams. This rapid drop in cross section is, of course, the result of a gauge cancellation as one expected from the standard model. Next, we see that except for f_8 and f_{10}, an anomalous form factor of order 1 will increase the high-mass W pair production cross section by at least an order of magnitude in the appropriately chosen θ^* region. This is usually the central region or near a dip in θ^* distribution. Finally, we notice that an anomalous f_i^Z in general produce a larger deviation than an anomalous f_i^γ, but otherwise, with very similar θ^* and M distribution. This may make separating the contributions from f_i^Z vs f_i^γ difficult.

Now let us discuss each anomalous form factor in the order of decreasing contributions to the high-mass W pair production. (By anomalous, we mean deviations from the corresponding standard-model values by 1.) From Figs. 9 and 10, we see that the contribution of an anomalous f_2 to (23) channel is greater than the corresponding standard model value by more than 3 orders of magnitude. Moreover, it keeps on increasing even when M reaches 550 GeV. Tree-level unitarity is badly broken and the γ_W^4 factor associated with f_2, as one can see from Eqs. (2.14) and (2.15), overwhelms the decrease in parton luminosity as M is increased. Next in line are the form factors f_7 and λ. f_7 contributes to (12) channel only while λ contributes to (11), (22), (13), and (23) channels. Their contributions are more than 2 orders of magnitude above the standard-model predictions for the transverse channels. The form factors f_4, f_5, f_6 contrib-

ute significantly only to the (13) and (23) channels. The deviations from the standard-model predictions are large only for high-mass (>300 GeV) W pairs and depend very much on the θ^* one chose. Note that the form factors f_3 and λ, for unit deviations from the standard-model value, give the same contribution to (13) and (23) channels. f_3 also contributes to (11), (22), (33) channels as does f_1. Their contributions are more than 1 order of magnitude above the standard-model values. Finally, among the three form factors f_8^Z, f_9^Z, f_{10}^Z, only f_9^Z contributes appreciably above the standard-model predictions to the high-mass W pair production cross section. Indeed its contribution to the (33) channel stays at about the same level even as M increases from 200 to 500 GeV.

As for the form factors associated with the neutral scalar-vector boson couplings, we find that an order one deviation from the standard-model value for these form factors produce, in most cases, no more than a factor of 2 increase in differential cross sections as is the case for f_8^Z and f_{10}^Z. This is expected as their contributions are suppressed by a factor of $(m_i/M)^2$, where m_i is the mass of the incoming fermions, while the probability of finding heavy quarks remain small for the values of M we considered at Tevatron energy. The contribution from f_9^Z is helped by a factor of ${\gamma_Z}^4$ which compensates for the decrease in heavy-quark luminosity.

As noted before in this paper we discuss only the polarization cross sections for W^+W^- pair production. To proceed to the correlations of the decay products of the W^+W^- is straightforward and the numerical results will be presented elsewhere.

In this work we have tried to get some idea of the numerical importance of the general three-vector couplings in a model-independent way. For specific models, there may exist relations among the various form factors making the effect smaller in some cases. This should be kept in mind in trying to derive constraints on the various form factors from the experimental data. A related point one should mention is that for the general three-vector-boson and neutral scalar-vector boson couplings we considered, tree-level unitarity is lost. This is the origin of some large effects we saw in the above discussions. For any realistic model, we expect tree-level unitarity to be restored at sufficiently high energies if perturbation theory is still valid. Insisting on tree-level unitarity will force certain relations among the various tri-vector-boson and scalar-vector boson couplings. The energy scale at which these relations are satisfied to a given precision is model dependent.

Now let us draw some conclusions based on the above discussion. At an integrated luminosity of 10 pb^{-1}, we expect, from standard-model prediction, to see no high mass (>300 GeV) central ($60^\circ \le \theta^* \le 120^\circ$) W^+W^- pairs events. Any such event signals new physics. If the new physics are due to anomalous tri-vector-boson couplings or Higgs-boson–vector-boson couplings which might arise, for example, from a new neutral gauge boson or neutral scalar, then our formalism can be applied to analyze such events. If the integrated luminosity can reach 100 pb^{-1}, we expect to see a few such events. They should come mainly from the (12) channel if standard model is correct.

It is very difficult to see at Tevatron energy any effects of the form factors whose contributions to the cross sections are proportional to the incoming quark masses. To test these form factors as well as to study in detail the polarization cross sections, one may have to wait for the next-generation machines such as the Superconducting Super Collider[32] or an upgraded high-luminosity Tevatron.

ACKNOWLEDGMENTS

We wish to thank E. Eichten and C. Quigg for valuable discussions, Y. P. Yao for careful reading of the manuscript and useful comments, and W. K. Tung for some useful conversations. We would also like to thank the Theory Group of Fermilab for hospitality. One of the authors (C.H.C.) would like to thank Y. P. Yao and G. L. Kane for helpful discussions and the High Energy Physics Theory Group of the University of Michigan, as well as the Theoretical Physics Group of LBL, University of California at Berkeley, for hospitality during his visits there.

*Present address: The Institute of Theoretical Physics, Academia Sinica, P.O. Box 2735, Beijing, China.

†On leave from The Institute of Physics, Academia Sinica, Taipei, Taiwan 11529, China.

[1]UA1 Collaboration, Phys. Lett. **122B**, 103 (1983); **126B**, 398 (1982); UA2 Collaboration, Phys. Lett. **122B**, 476 (1983); **129B**, 130 (1983).

[2]T. D. Lee and C. N. Yang, Phys. Rev. **128**, 885 (1962).

[3]W. A. Bardeen, R. Gastmans, and B. Lautrup, Nucl. Phys. **B46**, 319 (1972).

[4]W. Alles, Ch. Boyer, and A. J. Buras, Nucl. Phys. **B119**, 125 (1977).

[5]F. Bletzacker and H. T. Nieh, Nucl. Phys. **B124**, 511 (1977).

[6]R. W. Brown and K. O. Mikaelian, Phys. Rev. D **19**, 922 (1979).

[7]K. J. F. Gaemers and G. J. Gounaris, Z. Phys. C **1**, 259 (1979).

[8]M. Gourdin and X. Y. Pham, Z. Phys. C **6**, 329 (1980).

[9]M. Hellmund and G. Ranft, Z. Phys. C **12**, 333 (1982).

[10]R. W. Robinett, Phys. Rev. D **28**, 1192 (1983).

[11]K. O. Mikaelian, M. A. Samuel, and D. Sahdev, Phys. Rev. Lett. **43**, 746 (1979); R. W. Brown, D. Sahdev, and K. O. Mikaelian, Phys. Rev. D **20**, 1164 (1979).

[12]J. D. Stroughair and C. L. Bilchak, Z. Phys. C **26**, 415 (1984).

[13]Zhu Dongpei, Phys. Rev. D **22**, 2266 (1980).

[14]M. A. Samuel, Phys. Rev. D **27**, 2724 (1983).

[15]R. W. Brown, K. L. Kowalski, and S. J. Brodsky, Phys. Rev. D **28**, 624 (1983); S. J. Brodsky and R. W. Brown, Phys. Rev. Lett. **44**, 966 (1982).

[16]C. L. Bilchak, R. W. Brown, and J. D. Stroughair, Phys. Rev. D **29**, 375 (1984).

[17]B. Humpert, Phys. Lett. **135B**, 179 (1984).

[18]J. Stroughair and C. L. Bilchak, Z. Phys. C **23**, 377 (1984).

[19]C. L. Bilchak and J. D. Stroughair, Phys. Rev. D **30**, 1881

(1984).
[20]V. Barger, H. Baer, K. Hagiwara, and R. J. N. Phillips, Phys. Rev. D **30**, 947 (1984).
[21]D. A. Dicus and K. Kallianpur, Phys. Rev. D **32**, 35 (1985).
[22]W. J. Stirling, R. Kleiss, and S. D. Ellis, Phys. Lett. **163B**, 261 (1985).
[23]M. Tanimoto, Phys. Lett. **160B**, 312 (1985).
[24]M. Kuroda, J. Maalampi, D. Schildknecht, and K. H. Schwarzer, Phys. Lett. B **190**, 217 (1987); Nucl. Phys. **B284**, 271 (1987).
[25]J. F. Gunion and Z. Kunszt, Phys. Rev. D **33**, 665 (1986).
[26]E. Eichten, I. Hinchliffe, K. Lane, and C. Quigg, Rev. Mod. Phys. **56**, 579 (1984); **58**, 1065(E) (1986).
[27]M. J. Duncan, G. L. Kane, and W. W. Repko, Nucl. Phys. **B272**, 517 (1986).
[28]K. Hagiwara, R. D. Peccei, D. Zeppendfeld, and K. Hikasa, Nucl. Phys. **B282**, 253 (1987).
[29]J. Cortes, K. Hagiwara, and F. Herzog, Nucl. Phys. **B278**, 26 (1986).
[30]S. L. Glashow, Nucl. Phys. **22**, 579 (1961); S. Weinberg, Phys. Rev. Lett. **19**, 1264 (1967); A. Salam, in *Elementary Particle Theory: Relativistic Groups and Analyticity (Nobel Symposium No. 8)*, edited by N. Svartholm (Almqvist & Wiksell, Stockholm, 1968), p. 367.
[31]P. Q. Hung and J. J. Sakurai, Nucl. Phys. **B143**, 81 (1978); J. D. Bjorken, Phys. Rev. D **19**, 335 (1979); H. Fritzsch and G. Mandelbaum, Phys. Lett. **102B**, 319 (1981); L. Abbott and E. Farhi, *ibid.* **99B**, 69 (1981).
[32]Chao-Hsi Chang and S.-C. Lee, Phys. Lett. B (to be published).
[33]M. S. Chanowitz and M. K. Gaillard, Nucl. Phys. **B261**, 379 (1985); Phys. Lett. **142B**, 85 (1984); B. W. Lee, C. Quigg, and H. Thacker, Phys. Rev. D **16**, 1519 (1977).
[34]S. D. Drell and T. M. Yan, Ann. Phys. (N.Y.) **66**, 595 (1971).
[35]J. Frenkel, J. G. M. Gatheral, and J. C. Taylor, Nucl. Phys. **B223**, 307 (1984); G. Bodwin, Phys. Rev. D **31**, 2616 (1985); J. C. Collins, D. Soper, and G. Sterman, Nucl. Phys. **B261**, 104 (1985).
[36]J. C. Collins and W. K. Tung, Nucl. Phys. **B278**, 934 (1986); H. E. Haber, D. E. Soper, and R. M. Barnett, Report No. SCIPP-86/70, 1986 (unpublished).